Lawrence Berkeley National Laboratory
LBL Publications

Title
The Electrochemical Oxidation of Methanol on Tin-Modified Platinum Single Crystal Surfaces

Permalink
https://escholarship.org/uc/item/0dn9m4d8

Journal
Journal of physical chemistry, 95(9)

Authors
Haner, A.N.
Ross, P.N.

Publication Date
1990-11-01

eScholarship.org Powered by the California Digital Library
University of California

LBL-28399
Preprint

Lawrence Berkeley Laboratory
UNIVERSITY OF CALIFORNIA

Materials & Chemical
Sciences Division

Submitted to Journal of Physical Chemistry

The Electrochemical Oxidation of Methanol on Tin-Modified Platinum Single Crystal Surfaces

A.N. Haner and P.N. Ross, Jr.

November 1990

LBL-28399
Copy 2
| LOAN COPY |
|Circulates |
|for 2 weeks| Bldg. 50 Library.

Prepared for the U.S. Department of Energy under Contract Number DE-AC03-76SF00098

DISCLAIMER

This document was prepared as an account of work sponsored by the United States Government. While this document is believed to contain correct information, neither the United States Government nor any agency thereof, nor the Regents of the University of California, nor any of their employees, makes any warranty, express or implied, or assumes any legal responsibility for the accuracy, completeness, or usefulness of any information, apparatus, product, or process disclosed, or represents that its use would not infringe privately owned rights. Reference herein to any specific commercial product, process, or service by its trade name, trademark, manufacturer, or otherwise, does not necessarily constitute or imply its endorsement, recommendation, or favoring by the United States Government or any agency thereof, or the Regents of the University of California. The views and opinions of authors expressed herein do not necessarily state or reflect those of the United States Government or any agency thereof or the Regents of the University of California.

THE ELECTROCHEMICAL OXIDATION OF METHANOL ON TIN-MODIFIED PLATINUM SINGLE CRYSTAL SURFACES

Alexandra Norton Haner and Philip N. Ross

Materials and Chemical Research Division
Lawrence Berkeley Laboratory
Berkeley, CA 94720

To understand the role of tin as a promoter in the electrochemical oxidation of methanol, we have studied the geometric and electronic effect of tin atoms in different chemical states on/in the platinum surface by using single crystal faces of the ordered alloy Pt_3Sn and single crystal faces of pure Pt modified by electrodeposited/adsorbed tin, i.e. the so-called adatom state. We found that none of the alloy surfaces were more effective catalysts than any of the pure platinum surfaces under the conditions of measurement employed here, and that alloying platinum with tin to any extent significantly reduced the activity. As reported previously by others, we observed tin to spontaneously adsorb on platinum surfaces from dilute sulphuric acid supporting electrolyte containing Sn(II) in concentrations above ca. 5 μM. At a given concentration, the coverage by tin decreased as the atomic density of the platinum surface increased. However, we did not observe any enhancement of methanol oxidation on any platinum modified by this irreversibly adsorbed tin. We did observe a diffusion limited enhancement on Pt (111) and on Pt (100) due to Sn(II) in the electrolyte at 1 μM concentration. At this concentration, tin did not appear to be adsorbed to any observable extent, and the catalysis appeared to occur via the direct interaction of a dissolved tin species with the surface. We propose a mechanism of catalysis that is a hybrid homogeneous-heterogeneous sequence based on known homogeneous Pt-Sn catalysts.

This work was supported by the Assistant Secretary for Conservation of Renewable Energy, Deputy Assistant Secretary for Utility Technologies, Office of Energy Management, Advanced Utility Concepts Division of the U.S. Department of Energy under Contract No. DE-AC03-76SF00098.

INTRODUCTION

Methanol oxidation on pure platinum occurs at an overpotential 0.5-0.6 V above the thermodynamic potential (+0.043 V) for the oxidation of MeOH to CO_2 even for relatively low current densities, e.g. 0.1-1.0 mA/cm^2 [1]. To increase the efficiency of the methanol electro-oxidation reaction, it is necessary to find a more active catalyst. The most active catalysts for methanol oxidation currently known are either platinum catalysts promoted by electrodeposition of certain metals [2] or alloys of platinum such as Pt-Ru [3]. It has been reported that, above 40 ^{o}C, the methanol electro-oxidation reaction on tin-promoted catalysts in sulfuric acid solution proceeds at a current density that is 100x higher than on pure platinum [1,4] at the same overpotential, and appears to be one of the most active catalysts. The chemical state of tin in these catalysts was uncertain. Some studies have suggested the active state was metallic [6], i.e. a Pt-Sn alloy, while others have indicated the active state was an oxidized state [5,7].

To understand the role of tin as a promoter in the methanol oxidation reaction, we have studied the geometric and electronic role of the tin atom in two different chemical states. To this end, we conducted a series of electrochemical studies on the single crystal faces of ordered alloy Pt_3Sn and on the low index single crystal faces of platinum modified with electrodeposited tin, i.e. the so-called "adatom" state [2]. The crucial difference between the alloy and the adatom states is that in the alloy state, the tin atom is part of the bulk lattice while in the adatom state, it is not part of the bulk lattice, but is adsorbed on the surface with oxygenated ligands. As we show here, these two states differ not only in surface structure but

also in their effect on methanol electrocatalysis. In this paper, we present results on the surface composition and structure for platinum surfaces with electrodeposited tin; the surface composition and structure on the low index single crystals of the Pt_3Sn alloy are reported in another paper [8]. However, the kinetics of methanol oxidation on both types of surface are reported here.

EXPERIMENTAL

Single crystal Pt_3Sn was prepared by combining high purity platinum and tin in stoichiometric amounts and then refining the alloy using the Bridgeman technique. The formation of a single crystal, single phase alloy (fcc Cu_3Au structure, $L1_2$-type) was confirmed by x-ray diffraction analysis combined with Laue back-reflection x-ray diffraction. Once the homogeneity of the rod was determined, 1 mm single crystal samples oriented along the <111>, <110>, and <100> were spark cut and mechanically polished down to 0.05 μm [9]. All single crystal faces were within 0.5^{o} of their respective crystal planes as determined by Laue back-reflection x-ray diffraction.

All samples were gold brazed on to tantalum caps and mounted on to a sample holder with detachable Pt/10%Pt-Rh thermocouple leads. Electrochemistry, Low energy electron diffraction (LEED), and Auger electron spectroscopy (AES) experiments were conducted in a directly coupled electrochemical-UHV chamber [10]. Crystals were prepared with cycles of Ar^{+} sputtering, oxygen dosing, and vacuum annealing. Surface compositions were determined by use of AES with a single pass CMA (Varian CMA Model 981-2601) operated in the lock-in mode. The Auger peaks used for composition analysis were the Pt peak at 237 eV, the Sn

peak at 430 eV and the O peak at 510 eV. The peak-to-peak heights were measured using 5 V_{pp} modulation and a 3 kV electron beam. The surface structure was determined using 4-grid LEED optics (Varian Model 981-2148).

Aqueous hydrofluoric (HF) and sulfuric acid (H_2SO_4) solutions were prepared using HF (Ultrex Grade, JT Baker) and H_2SO_4 (Ultrex Grade, JT Baker), respectively. The water used was pyrolytically triply distilled water (TDW). Tin(II) solutions were prepared using H_2SO_4 and SnF_2 (Cerac, 99.9% pure). To minimize contamination, all solutions were prepared on the same day as the experiments and were changed with each new experiment. A Pt disk/Au ring assembly was used as the auxiliary working/counter electrode system onto which a 100 μl drop of electrolyte was delivered via a PTFE capillary. All teflon and Kel-F pieces were cleaned with concentrated HF, neutralized with 30% potassium hydroxide, and then boiled in TDW for several hours. The reference electrode used was a Pd-H wire which was charged vs. the Au ring. However, all potentials quoted in this paper will be vs. a reversible hydrogen electrode (RHE) in the same electrolyte (1 atm. H_2). All electrolytes were continuously deaerated with helium gas. Unless otherwise stated, all electrode emersions (removal of the electrode from solution) were accomplished under potentiostatic control at 0.4 V. Details of the emersion procedure and transfer to the UHV chamber are described in [10]. No rinsing was employed. Electrolyte adhering to the electrode was removed by exposure to vacuum.

After transfer of the crystal from the UHV system [10], the crystal was contacted with electrolyte while potentiostatted at 0.4 V using a 1 MΩ shunt resistor wired in parallel. After contact, with a

delay of less than 10 seconds, the potential was swept cathodically usually to about 0 V, then reversed for an anodic sweep to the selected anodic reversal potential. For the methanol kinetic measurements, the voltammogram taken as the measurement was typically the second anodic/cathodic sweep after contact.

RESULTS

I. Pt_3Sn Alloy

A. The <111> face

The Pt_3Sn (111) face exhibited a p(2x2) LEED pattern which corresponds to the real space structure shown in Figure 1, with every tin atom surrounded by six platinum atoms and a surface concentration of 25% Sn. We expected that such an ensemble would be quite active for methanol oxidation. Comparing the Pt_3Sn (111) voltammogram with that for Pt (111) (Fig. 2) indicates two new features appearing for the alloy surface: a reversible process (I) at ca. 0.35 V and another reversible (but kinetically hindered) process (II) at ca. 0.7 V. The amount of adsorbed hydrogen (charge under I') is about the same on both surfaces, but the sulfate adsorption feature (II') unique to Pt (111) [11] is not present on Pt_3Sn (111). The voltammetry curve shown in Fig. 2 was stable with repeated cycling within this potential region. Emersion of the crystal at any potential in this region and analysis by AES indicated there was neither Sn loss from the surface, nor was there a significant oxygen AES signal, indicating the Sn remained in a metallic alloyed state after voltammetry. AES analysis did indicate the possibility that peak I on Pt_3Sn (111) may be due to sulfate adsorption. Comparison of the voltammograms with and without methanol (Fig. 3)

indicates only a small difference between the two, and that the Pt_3Sn (111) surface is a very poor catalyst for methanol oxidation. Comparison with Pt (111) indicates the presence of tin atoms in this form actually decreased the activity of pure Pt. We interpreted this suppression of the methanol oxidation reaction to be due to a possible partial blocking of Pt sites by HSO_4^- adsorbed on nearest-neighbor tin atoms, and by an electronic effect of intermetallic bonding on methanol adsorption.

To eliminate the possible role of the bisulfate anion, we studied the kinetics of methanol oxidation in 0.3 M HF (pH = 2). The fluoride anion is known to be a weakly adsorbing anion on Pt and on many other metals due primarily to very strong solvation in aqueous solution. However, tin is complexed by fluoride and may be expected to dissolve more readily in HF than in H_2SO_4 [12]. Cyclic voltammetry with successively increasing anodic limits with the same electrode ("window-opening" voltammetry) for the Pt_3Sn (111) crystal face in HF is shown in Fig. 4. One can see a reversible redox couple at 0.34 V, at the same potential as in H_2SO_4, and an irreversible process occurring above 0.7 V, which AES analysis of the emersed crystal indicated was Sn dissolution. With the addition of Sn(II) to the solution, dissolution was retarded and a reversible process appeared that was similar to that observed on the alloy in H_2SO_4. In HF, the reversible feature at 0.34 V, which we will call the Pt_3Sn alloy peak, is much better defined than in H_2SO_4. We also note that the feature at 0.34 V was only observed when the Pt_3Sn crystal produced a sharp p(2x2) LEED pattern; e.g. a sputtered but not annealed surface, which is depleted of Sn, never produced this feature. The kinetically hindered surface process at 0.6-0.8 V appears in the same potential region as the process arising from

Sn adsorbed on Pt (111) in H_2SO_4, to be described in a later section. The voltammogram of the Pt_3Sn (111) alloy with methanol in 0.3 M HF can be seen in Fig 5. Although some methanol oxidation current is observable in HF, no enhancement is indicated when comparing the Pt_3Sn (111)/MeOH/HF cyclic voltamogram with the Pt (111)/MeOH/HF voltammogram; in fact the alloy is much less active.

B. The <100> face

We have observed that the composition and structure of the Pt_3Sn (100) surface can be modified depending on the surface preparation conditions [8]. We found that there is preferential termination of the [100] oriented crystal to form surfaces that have a step-terrace structure with mixtures of (100) terraces (50% Sn) and (200) terraces (100% Pt) connected by multi-atomic steps. At an annealing temperature less than 400 ^{o}C, the predominant LEED pattern observed was (1x1) indicative of a predominance of (200) terraces. Above 400 ^{o}C, the predominant LEED pattern observed was c(2x2) indicative of a predominance of (100) terraces.

The cyclic voltammetry of the Pt_3Sn (100) c(2x2) alloy in H_2SO_4 was very similar to that for the Pt_3Sn (111) surface; i.e. with the addition of methanol no significant change in the voltammogram could be observed (Fig. 6). Although the results with Pt_3Sn (100)-c(2x2) are similar to the (111), it should be noted that the peaks for the (100) surface are slightly cathodic of those observed on Pt_3Sn (111). Because of the increase in the platinum concentration (from 50% to 90%) of the Pt_3Sn (100)-(1x1) surface, the resulting cyclic voltammograms in H_2SO_4 are very different from the c(2x2) surface. The first peak at 0.2 V is the same hydrogen adsorption peak observed on all Pt (100) vicinal

surfaces [13]. The second peak at 0.7 V appears similar to the peak attributed to Sn that was observed on the (111) and (100)-c(2x2) surfaces. Figure 6 also shows the cyclic voltammogram with methanol. One can clearly see that the increase in platinum surface concentration produced a concomitant increase in methanol oxidation current.

A window opening experiment on the Pt_3Sn (100) c(2x2) crystal was also conducted in HF. Similar behavior to the Pt_3Sn (111) face in HF is observed. On the first sweeps, suppression of hydrogen adsorption/desorption peaks characteristic of Pt is apparent. The process at 0.35 V, which we associated with Sn in the alloy state on the Pt_3Sn (111) surface, is absent. The irreversible process we identified by AES as tin dissolution was observed at potentials 0.15 V-0.2 V cathodic of those on Pt_3Sn (111). As for the (111) surface, cycling to successively more anodic potential increased the hydrogen adsorption/desorption charge at 0.2 V, showing clearly that suppression of hydrogen adsorption is due to the presence of tin in the alloy surface. In the presence of methanol, as with the (111) surface, the oxidation current increased concomitently with the decrease in Sn concentration in the surface.

C. Polycrystalline 2% Sn Alloy

A polycrystalline alloy containing ca. 2% Sn in the bulk crystal was studied using the same procedures as used to study the Pt_3Sn single crystals. AES analysis indicated that surface segregation of tin occurred to produce a surface concentration of ca. 10% tin. However, the electrochemistry results were similar to those observed on the single crystals of Pt_3Sn; i.e. there was no observable enhancement in methanol oxidation current with this alloy versus a polycrystalline

platinum surface, even though the surface concentration was only 10% vs. 25-50%.

II. Tin modified Platinum Surfaces

A. The <111> face

The Pt (111) crystal produced a $(\sqrt{3}x\sqrt{3})R30^{o}$ LEED pattern when emersed from 5 mM H_2SO_4 containing Sn(II) in concentrations ranging from 8-16 μM. The pattern was not observed in the absence of tin. The $(\sqrt{3}x\sqrt{3})R30^{o}$ pattern is interpreted as a tin adatom occupying every third lattice site of the Pt (111) surface unit mesh, i.e. a Sn/Pt atomic ratio of 0.33. This particular tin adatom/Pt (111) state appears to correspond to a tin species spontaneously adsorbed on the Pt (111) crystal face from this Sn(II)/H_2SO_4 solution, since the amount of tin on the surface was independent of the potential of emersion. A similar spontaneous adsorption of tin from sulfuric acid was previously observed by Bittins-Cattaneo and Iwasita [14] and Sobkowski, et al. [15] on polycrystalline Pt electrodes.

In terms of electrochemistry, two features dominate the voltammogram of Pt (111) in this Sn(II)/H_2SO_4 electrolyte (12 μM Sn(II), 5 mM H_2SO_4, pH = 2, Fig. 7): one at 0.5 V (I) and the other at 0.8 V (II). We suggest that feature I is the anion adsorption process unique to Pt (111) in dilute H_2SO_4 [11] and that feature II is a surface redox process that appears to be associated with the tin species that spontaneously adsorbs on Pt (111) from H_2SO_4 [14-15]. Experimental support for association of features I and II with an adsorbed species on the Pt (111) surface can be seen from a scan rate (υ) dependence study of the two peaks (Fig. 7, right). Both show a <u>linear</u> dependence of the

peak current with scan rate, indicating a surface process (versus $\sqrt{v}$ dependence for diffusing species) [16a].

The effect of this adsorbed tin on the methanol oxidation rate on Pt (111) in sulfuric acid can be seen in Fig. 8 (left). A decrease in the rate of reaction occurred with the addition of tin at 12 μM Sn(II) and higher. As the solution tin concentration decreased from 12 μM, the methanol oxidation rate increased as the amount of irreversibly adsorbed tin detected by AES decreased linearly (Fig. 9). Actual enhancement of the rate relative to the rate without Sn in solution occurred at Sn(II) concentration between 0.5-5 μM. Maximum enhancement of the methanol oxidation reaction occurred at 1 μM Sn(II). This suggests that the enhancement at 1 μM Sn(II) occurs specifically by interaction with atomically flat (111) terraces of the Pt (111) crystal. This was seen by repeating the experiment with a roughened Pt (111) surface, i.e. one that has been Ar^+ bombarded but not annealed. As seen in Fig. 8 (right), there was no enhancement with the addition of 1 μM Sn(II).

The scan rate dependence of the methanol oxidation currents on the pure Pt (111) and tin-modified Pt (111) surfaces was examined using 5 mM H_2SO_4 and 3 different CH_3OH concentrations (0.025, 0.1, and 1 M). For the pure Pt (111) surface, the methanol oxidation currents on the anodic sweep were independent of sweep rate, and were approximately half-order in CH_3OH concentration. However, when modified by 1 μM Sn(II) in solution, the methanol oxidation currents varied with $\sqrt{v}$ (Fig. 10) indicating that with the addition of tin, the reaction becomes diffusion limited. Calculation of the diffusion limited current from LSV theory applied to a generic half-order reaction [16b] indicates CH_3OH, and not Sn(II), to be the diffusion limiting species. Thus, the true kinetic

enhancement by tin atoms interacting with the Pt (111) surface is at least the factor of 3, as shown in Fig. 9.

B. The <110> face

The voltammetry of UHV clean and annealed Pt (110) in 5 mM H_2SO_4 containing 25 mM CH_3OH is shown in Fig. 11. With the Pt (110) surface, we observe an 8x enhancement over Pt (111) in the methanol oxidation rate in the potential region 0.6-0.8 V on the first anodic sweeps after immersion. A similar enhancement was also observed by Clavilier, et al. [17]. As reported by Clavilier and co-workers, this enhancement is time-dependent; the high activity of the (110) face decreases in proportion to the time the potential is maintained in the hydrogen adsorption region, i.e. the "autopoisoning" phenomenon [17], which is more pronounced for (110) than (111).

The effect of tin on the methanol oxidation rate with the Pt (110) surface is shown in Fig. 11. Interestingly, the addition of 12 μM Sn(II) suppressed the reaction ten-fold and shifted the peak potential > 0.2 V anodic of that observed without tin. At no solution tin concentration did we see an enhancement of the methanol oxidation reaction. At a solution concentration of 0.5 μM Sn(II) or lower, the methanol oxidation current was the same as without Sn(II) added to the electrolyte.

On both the Pt (110) and Pt (111) faces, the Sn/Pt AES ratio varied linearly with the solution tin concentration (Fig. 9). In both cases, the slopes (Δ (Sn/Pt) AES ratio/Δ [Sn(II)]) were similar; however, the intercepts were different. On Pt (110), the Sn/Pt AES ratio extrapolates to zero at 0.5 μM Sn(II), while on Pt (111) the Sn/Pt AES ratio becomes zero at 5 μM Sn(II). We suggest that this order of

magnitude difference is due to the difference in the point of zero charge of the two crystal faces.

C. The <100> face

After contact with the sulfuric acid electrolyte, the UHV reconstructed (100)-(5x20) pattern was transformed back to a (1x1) LEED pattern. This transformation was reported before for Pt (100) [13] and Au (100) [18] and appears to be driven by anion adsorption [19]. Emersion of Pt (100) from tin containing electrolyte produced a c(2x2) pattern for Sn (II) concentrations above ca. 5 μM. As with the (111) and (110) surfaces, this adsorbed state of Sn appears to be an oxygen complex. This is clearly seen from the AES Sn/Pt and O/Sn peak ratios reported in Table I, where the O/Sn ratio was an essentially constant value (0.75 ± 0.1) for all tin coverages. Using standard sensitivity factors from the Auger Handbook [20], we calculate this O/Sn AES ratio to be consistent with the 1:1 stoichiometry of the $Sn(OH)^+$ species proposed by Bittens-Cattaneo and Iwasita [14].

On the Pt (100) face, the Sn/Pt AES ratios did not vary linearly with the solution tin concentration (Fig. 9) as they did for the (111) and (110) surfaces. Beginning at 1 μM Sn(II), the Sn/Pt AES ratio increased linearly and then began to level off at 6 μM Sn(II), with a Sn/Pt AES ratio of ~1.2. From the c(2 x 2) LEED pattern, this saturation coverage appears to correspond to a Sn/Pt atomic ratio of ~0.25. The effect of Sn(II) in solution on the methanol oxidation kinetics on Pt (100) were similar to the results with the Pt (111) surface, i.e. maximum enhancement occurred at 1 μM Sn(II).

D. Polycrystalline Pt

The kinetic results on polycrystalline platinum were similar to the data for the (110) surface in that no significant enhancement of the methanol oxidation reaction was observed with the addition of tin. However, the variation of the Sn/Pt AES ratio with the solution tin concentration was not the same as Pt (110) (see Fig. 9), but appeared to be more like a sum of (111) and (100) isotherms. Nonetheless, the kinetics of methanol oxidation in the presence of tin were unlike those observed on either the (100) or (111) faces.

DISCUSSION

The results of methanol oxidation kinetics on the Pt-Sn alloy surfaces were disappointing from a practical standpoint, but have interesting implications for electronic theories of catalysis. It was clear that the activity of the Pt_3Sn alloys increased when tin was anodically removed from the surface, yet none of the alloy surfaces, even the dilute polycrystalline alloy with only 10% tin in the surface, approached the activity of pure Pt surfaces. Because tin had a strong negative effect on the catalysis even when the concentration of tin in the surface was relatively low (e.g. 10%), it appears that the effect of tin must be primarily an electronic effect. There is ample precedent for a strong electronic effect of intermetallic bonding on the adsorption energy of CO on Pt surfaces [21], so an electronic effect on the adsorption of methanol on the Pt sites due to intermetallic bonding with neighboring (including subsurface) tin atoms is a reasonable conclusion.

The difference in the hydrogen adsorption region between the Pt_3Sn alloy and the pure Pt surfaces is interesting, but difficult to interpret based on voltammetry alone. On the (111) alloy surface in H_2SO_4, there was some indication by AES that the feature labeled I in Fig. 2 was due to sulfate adsorption, but when this surface was examined in HF, the feature was even better defined. Kinetically, the process for I appears very hydrogen-like, showing no peak shift even to very high sweep rates, and we were tempted to postulate that this feature is due to a unique strongly bound state of hydrogen on the Pt_3Sn (111) alloy surface. However, the hydrogen-like capacitance appears to be strongly <u>suppressed</u> (nearly zero) on the (100)-c(2x2) surface, so if the process were hydrogen adsorption on Pt-Sn alloy, it would have to be extremely sensitive to the surface composition and structure. Further, the charge under peak I, ca. 70 $\mu C/cm^2$, does not appear to be consistent with a high heat of adsorption, which is indicated by the potential of peak I to be ca. 32 kcal/mol (≡ 2FV). Normally we associate strongly adsorbing states with high coverage, unless the states occur only at specific sites on the surface. It would be very unusual for a single-crystal metal surface to have only a few strongly adsorbing sites (~ 30 kcal/mol) and <u>also</u> only a small number of more weakly adsorbing sites (~ 10 kcal/mol), which would be the result of a hydrogen interpretation. An alternative, but still problematic interpretation, is that in <u>both</u> H_2SO_4 and HF, this peak is pseudo-capacitance from specific adsorption of the acid anion. Tin is strongly complexed by F^-, forming SnF_4^{2-} and SnF_6^{2-} as the primary species of Sn(II) and (IV) in HF [12]. Thus it is reasonable to suggest that there is a specific adsorption step preceeding complexation and dissolution. However, there was no evidence

of F^- adsorption observed by AES analysis of electrodes emersed from HF, so we have no direct evidence to support the anion adsorption supposition.

The experimental apparatus used in this study is ideally suited for studying alloy and admetal electrochemistry, in that it combines the powerful UHV techniques of LEED, LEISS, and AES to determine the structure and composition of the surfaces being examined electrochemically. However, these advantages are not obtained without some experimental limitations. In our system, we have found that one is limited to voltammetric techniques employing reactants in relatively dilute concentration (mM) and experiments of relatively short duration (<1000 sec). Thus the kinetic results must be interpreted recognizing the limitations of the voltammetric technique for kinetic analysis and the difficulty of studying reactions that may be time dependent. The latter is particularly important in the case of methanol oxidation, as it is usually postulated that methanol reactions on Pt surfaces proceed via two parallel pathways [22],

$$CH_3OH \begin{cases} \nearrow \text{ Bulk products, e.g. } CO_2, HCOOH, HCOH \\ \searrow \text{ Surface products or "poisons"} \end{cases}$$

The accumulation of "poisons" is a relatively slow process on most Pt surfaces [23], with a time constant longer than the duration time in our experiments. We have, therefore, structured our experiments to examine the kinetics in the absence of accumulated "poisons", and the voltammetric technique is advantageous in this respect. The

difficulties with the voltammetric technique are that the correction of the observed current for the contribution from adsorptive processes to obtain the faradaic current for methanol oxidation [16] can introduce large errors, and the presence of a diffusional limitation complicates the analysis even further. We found these difficulties to be so severe as to limit the kinetic analysis to a qualitative level. That is, the presence of tin clearly increases the rate of methanol oxidation on the (111) surface of Pt, and the enhancement is at least of a factor of 3, but the sweep rate dependence of the enhancement, and the probable diffusional limitation at these dilute concentrations, indicates the true kinetic enhancement could be much larger. Furthermore, this enhancement applies only to "fresh" surfaces, and is limited to surfaces which have experienced only a few sweeps through the potential region where "poisons" might be generated. With our apparatus, we were not able to make a systematic and satisfactory study of the catalysis of "aged" surfaces, which could be more representative of the catalysis in fuel cells [24]. It may even be the case that our observation of anti-catalysis associated with tin in some experiments, e.g. tin adsorbed on Pt (110) and all the Pt-Sn alloy surfaces, would not apply to "aged" catalysts.

A number of theories have been proposed to explain the catalytic effect of tin on platinum. Cathro [5] suggested that $Sn(OH)_4$ was oxidizing the "adsorbed methanol" intermediate. However, this mechanism was challenged by Janssen and Moolhuysen [6]. Instead, they postulated that zero-valent tin atoms electronically affected the adsorption properties of methanol on the platinum atoms via a "ligand effect". This effect would result in weaker bonding of the methanol intermediate

to the platinum surface and facilitate the coadsorption of water to produce carbon dioxide. Another explanation by Motoo and co-workers [25] suggested that a tin-oxide complex could provide an oxygen atom to form carbon dioxide from methanol at relatively low potentials. Still another explanation, called the "third body effect", was put forward by Angerstein-Kozlowska, et al. [26] and by Beden, et al. [27]. They postulated that adsorbed tin hindered the formation of organic residues ("poisons") by blocking platinum sites. However, this explanation is also challenged [14,28-29]. Two recent papers support the mechanism of Motoo and co-workers. Bittins-Cattaneo and Iwasita [14] suggested that the catalytic effect of tin may be due to a $[Sn(II)OH]^+$ surface species which could provide oxygen atoms for the oxidation for methanol to carbon dioxide at potentials 0.15 V lower than that observed on pure platinum. Support for the presence of a catalytic effect from an adsorbed divalent tin species has also been presented by Sobkowski, et al. [15] in an elegant radiotracer experiment.

Our results from the study of Pt-Sn alloys clearly indicated that there is no Pt-Sn alloy of any composition that is more active than pure Pt under the conditions of catalysis used here, which is contrary to the conclusion made by Janssen and Moolhuysen [6] under fuel cell conditions. However, the voltammetry data we reported here, and unpublished photoemission measurements in our laboratory, do support the conclusion that there is a very strong "ligand effect" on the way methanol adsorbs on the Pt surface due alloying the Pt with Sn, but this effect is <u>not beneficial</u> for catalysis under our conditions of testing. It may be that under fuel cell conditions of steady-state electrolysis,

the "ligand effect" may reduce the accumulation surface residues and thus improve the catalysis observed under those conditions.

We did observe a strong catalytic effect on Pt(111) and on Pt(100) in H_2SO_4 electrolyte upon addition of Sn(II) to the electrolyte. However, the maximum effect occurred at a solution concentration of 1 μM Sn(II). Emersion of these crystals from this electrolyte and examination of the surface coverage by AES indicated the Sn concentration to be so low as to be essentially undetectable. Furthermore, at the level of 1 μM, the presence of tin in the electrolyte was virtually undetectable in the cyclic voltammetry of Pt (111) (!). Thus, the chemisorbed Sn species which forms on the (111) surface at higher concentration, and on the (110) and (100) surfaces at all concentrations, is the Sn species detected by LEED/AES analysis of emersed electrodes, and is <u>not</u> the catalytically active species of Sn, i.e. the active species is a reversibly adsorbed state that cannot be emersed from a Sn/H_2SO_4 electrolyte. Other investigators have reported that a Pt surface can be emersed from a Sn/H_2SO_4 electrolyte, immersed in an H_2SO_4 electrolyte without Sn, and observe an enhancement of methanol catalysis [14-15]. When we attempted this same experiment, no enhancement was observed unless the surface was "activated" by anodization above 1.0 V, where desorption of the irreversibly adsorbed Sn occurred. Since no Sn is present in the electrolyte initially, desorbed Sn diffuses away from the surface, creating a very dilute Sn-containing electrolyte and a tin-free Pt surface. We suggest that other workers employing anodic cycling [14-15] possibly achieved the same effect in their experiments.

We have no direct evidence of the mechanism of action of Sn added to the acid electrolyte on the rate of methanol oxidation on Pt (111) and Pt (100). The following is, therefore, a hypothesis based on the results here and previously suggested mechanisms. It appears from our results that the active state of tin is a dissolved species which interacts weakly with the Pt surface. Stronger interaction, such as chemisorption onto Pt surfaces having open atomic structures, like (110) or a roughened (111) surface, did not produce enhanced catalysis. How then does a dissolved species that is weakly interacting with a surface affect catalysis at that surface? We suggest that the redox mechanisms postulated in many earlier studies can be married to the mechanism of Pt-Sn homogeneous catalysis [30] to give a plausible hybrid mechanism, such as,

$$CH_3OH + Pt \Longrightarrow (HCO)_{ads} + 3H^+ + 3e$$

$$(HCO)_{ads} + SnX_4\,(OH)_2^{2-} \Longrightarrow CO_2 + SnX_4^{2-} + H_2O + H^+ + 1e^-$$

$$2H_2O + Pt \Longrightarrow 2(OH)_{ads} + 2H^+ + 2e^-$$

$$2(OH)_{ads} + SnX_4^{2-} \Longrightarrow SnX_4\,(OH)_2^{2-}$$

The ligand X is probably bisulphate and/or chloride, the latter being a known impurity in our electrolyte present at about the same level of concentration as the added Sn. Chloride is the preferred ligand in Sn homogeneous catalysts [30], whereas a hydrido-bisulphate complex is known [31] for tin dissolved in sulfuric acid. It is seen from the above mechanism that the dissolved tin complex can enhance the reaction between two strongly adsorbed relatively immobile species by serving as a mobile intermediate. Note also that this mechanism does not activate water at a lower potential than pure Pt, in agreement with our observation that tin did not change the potential of onset for methanol

oxidation on any of the Pt crystal surfaces. This mechanism, if correct, suggests that a totally new approach combining concepts of homogeneous and heterogeneous catalysis might lead to improved new catalysts for methanol electrooxidation.

ACKNOWLEDGMENTS

This work was supported by the Assistant Secretary for Conservation of Renewable Energy, Deputy Assistant Secretary for Utility Technologies, Office of Energy Management, Advanced Utility Concepts Division of the U.S. DOE under Contract No. DE-AC03-76SF00098. We would like to thank Mr. Larry Jones (Ames Laboratory) for the preparation of the Pt_3Sn single crystal boule. We would like to thank Professor Dennis Evans (University of Delaware) for providing us with current-potential curves for LSV with non-unity reaction order.

FIGURE CAPTIONS

[1] Real space structures corresponding to different bulk terminations normal to the <111>, <100>, and <110> crystal planes of Pt_3Sn.

[2] Cyclic voltammograms of Pt_3Sn (111) and Pt (111) in 5 mM H_2SO_4 (--- Pt_3Sn and —— Pt).

[3] Cyclic voltammograms of Pt_3Sn (111) in 5 mM H_2SO_4 with (- - -) and without 25 mM CH_3OH (——).

[4] Pt_3Sn (111) (left) and Pt_3Sn (100) (right) window opening in 0.3 M HF.

[5] Cyclic voltammograms of Pt_3Sn (111) (- - -) and Pt (111) (——) in 25 mM CH_3OH and 0.3 M HF.

[6] Anodic sweeps of Pt_3Sn (100) c(2x2) in 5 mM H_2SO_4 with (---) and without 25 mM CH_3OH (——) (left). Anodic sweeps of Pt_3Sn (100) (1 x 1) in 5 mM H_2SO_4 with (---) and without 25 mM CH_3OH (——) (right).

[7] Cyclic voltamogram of Pt (111) in 5 mM H_2SO_4 with (——) and without (- - -) 12 μM Sn(II) (left) and scan rate dependence study of the peak current of peaks I and II (right).

[8] Anodic sweeps of Pt (111) in 5 mM H_2SO_4 and 25 mM CH_3OH with varying concentrations of tin (—— no tin, --- 1 μM Sn(II), - · - 12 μM Sn(II) (left). Cyclic voltamogram of Ar^+ bombarded Pt (111) in 5 mM H_2SO_4 and 25 mM MeOH with (---) and without (——) 1 μM Sn(II) (right).

[9] Plot of Sn/Pt AES ratio vs. solution tin concentration (*** Pt(111), ooo Pt(110), xxx Pt(100), +++ Poly Pt).

[10] Sweep rate dependence of the anodic current for methanol oxidation (corrected for capacitance) on Pt (111) in 25 mM CH_3OH with

(left) and without (right) 1 μM Sn(II) added to the electrolyte.

[11] Anodic sweeps of Pt (110) in 5 mM H_2SO_4 and 25 mM CH_3OH without tin (——) and with 12 μM Sn(II) (- - -).

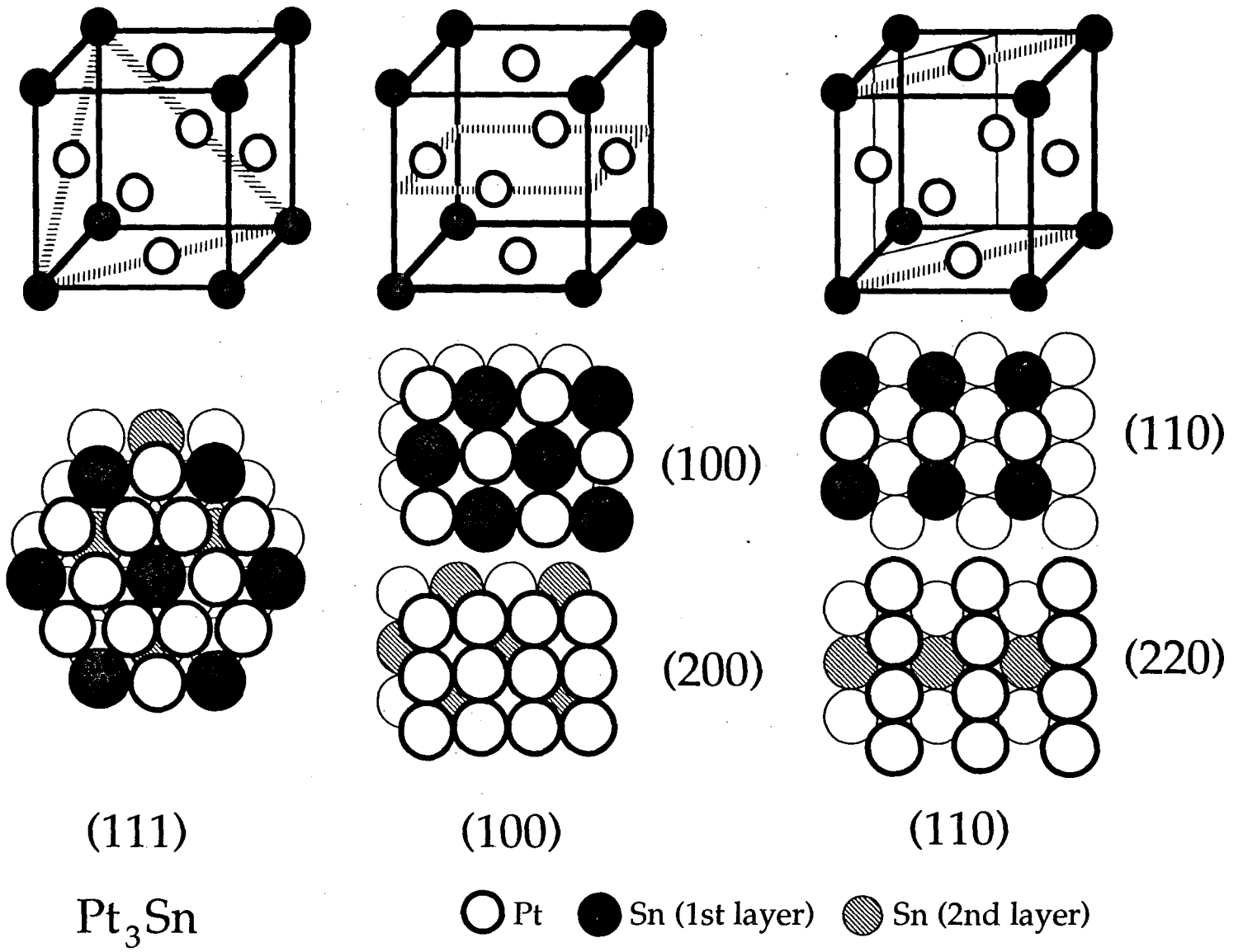

XBL 907-2424

Fig. 1

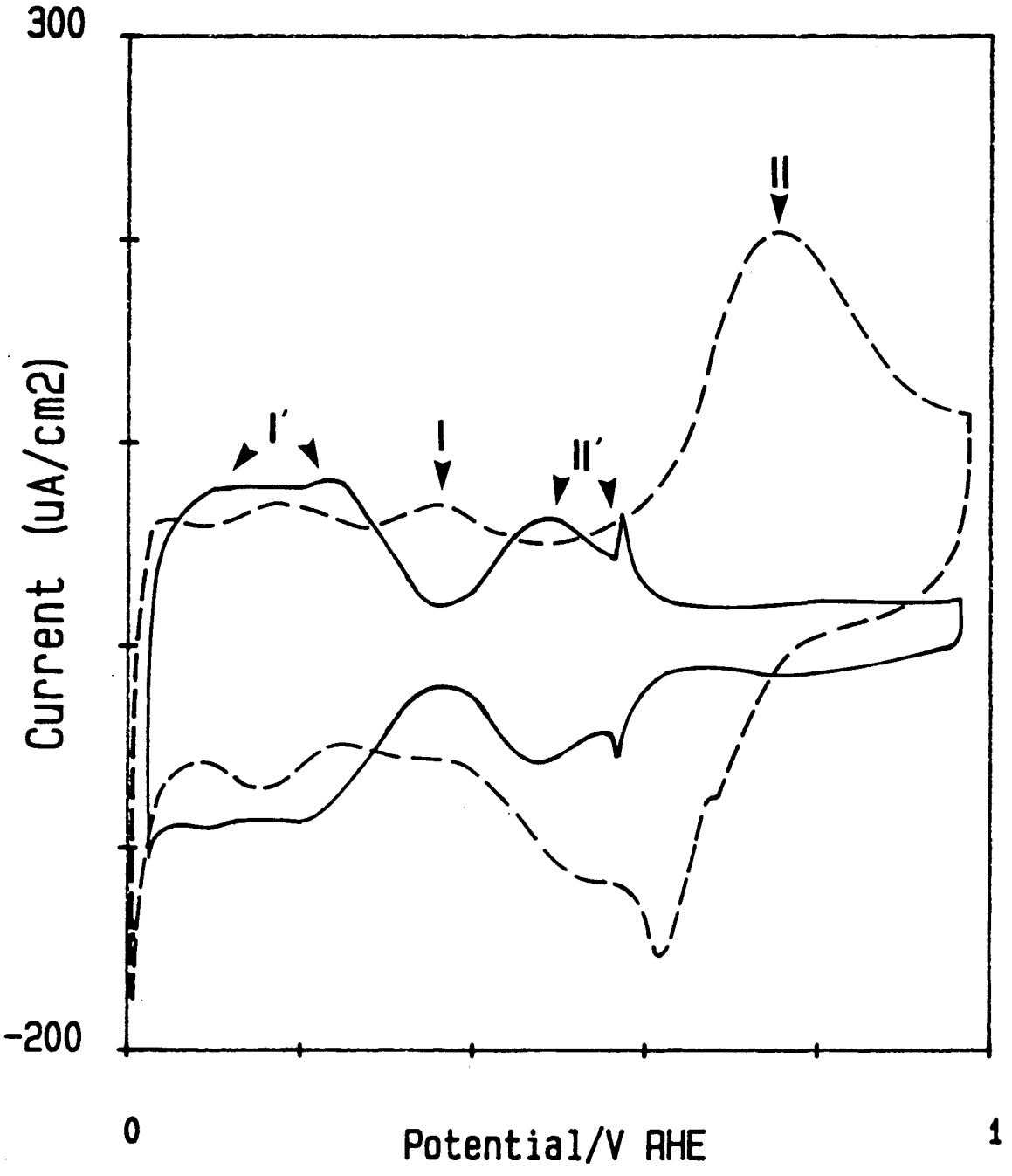

XBL 905 – 6370

Fig. 2

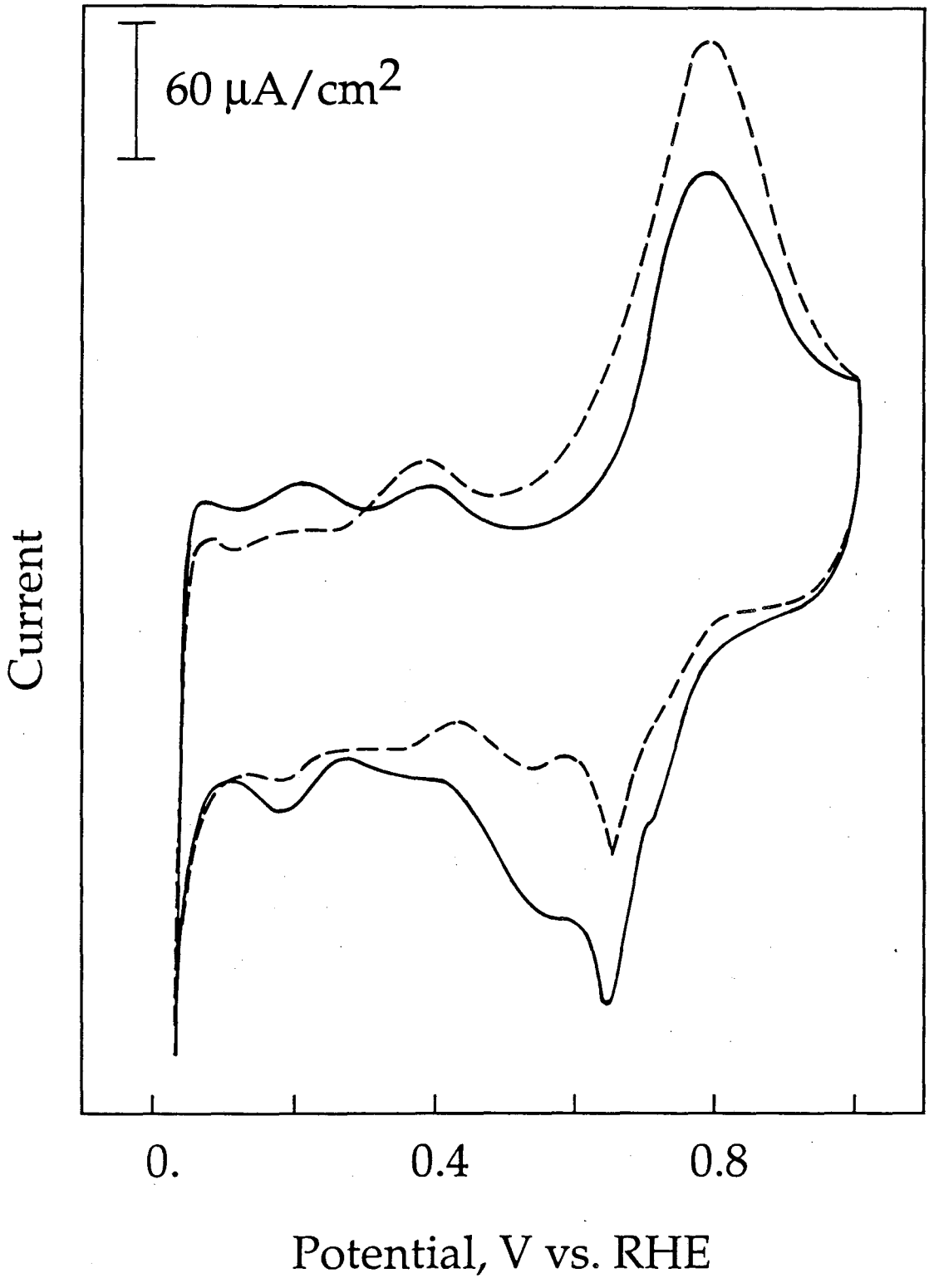

XBL 904 – 6360

Fig. 3

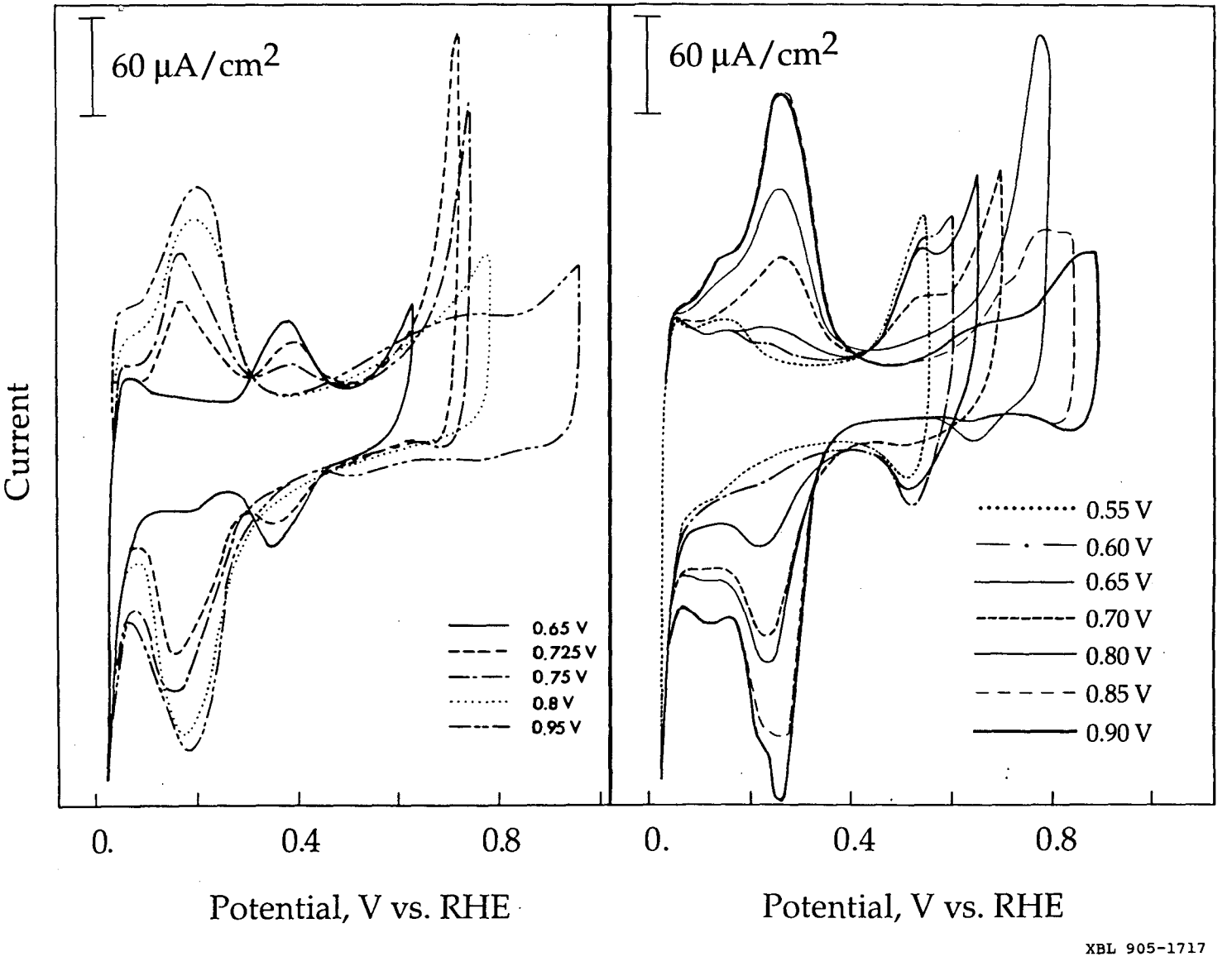

XBL 905-1717

Fig. 4

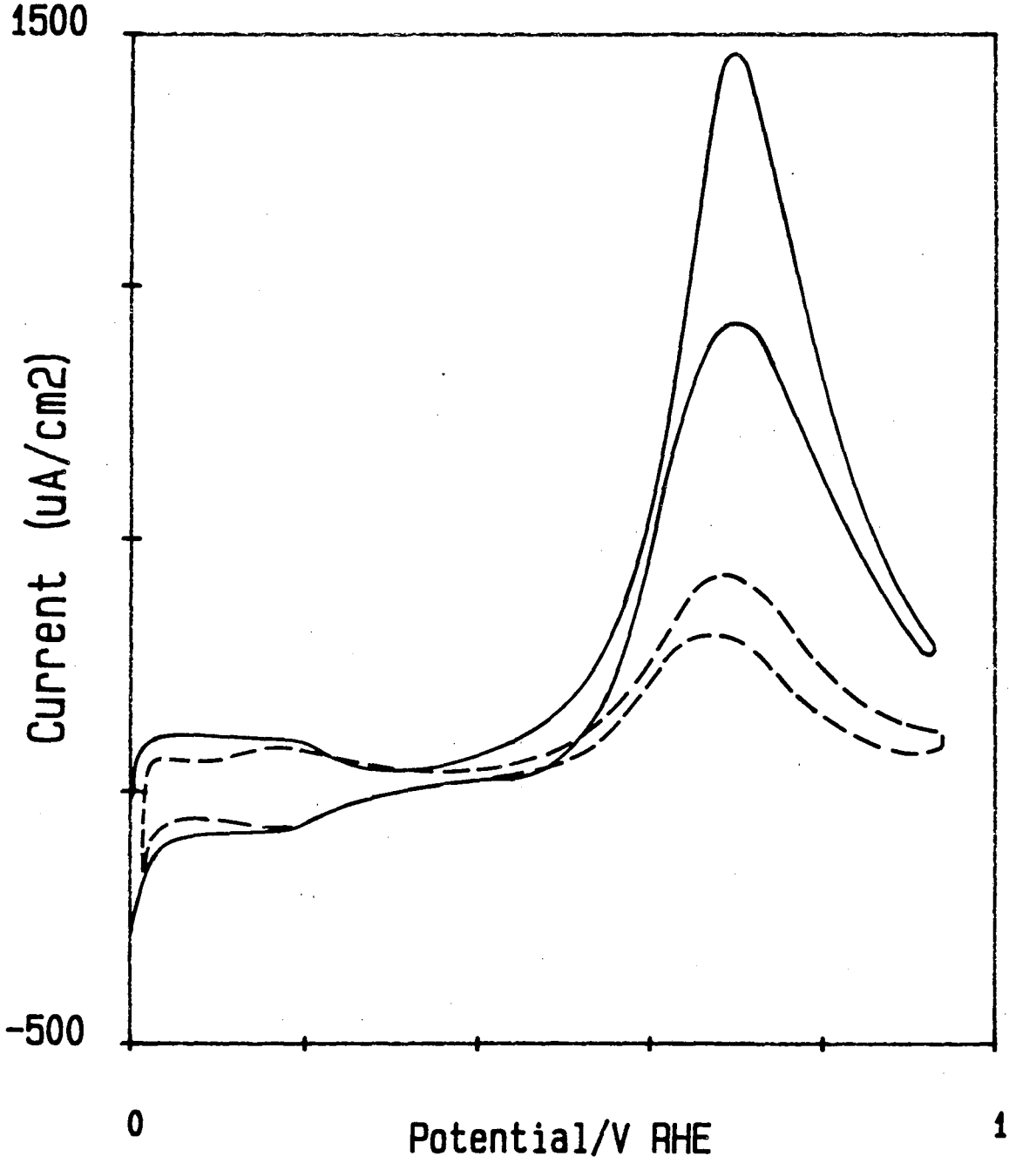

XBL 905 – 6371

Fig. 5

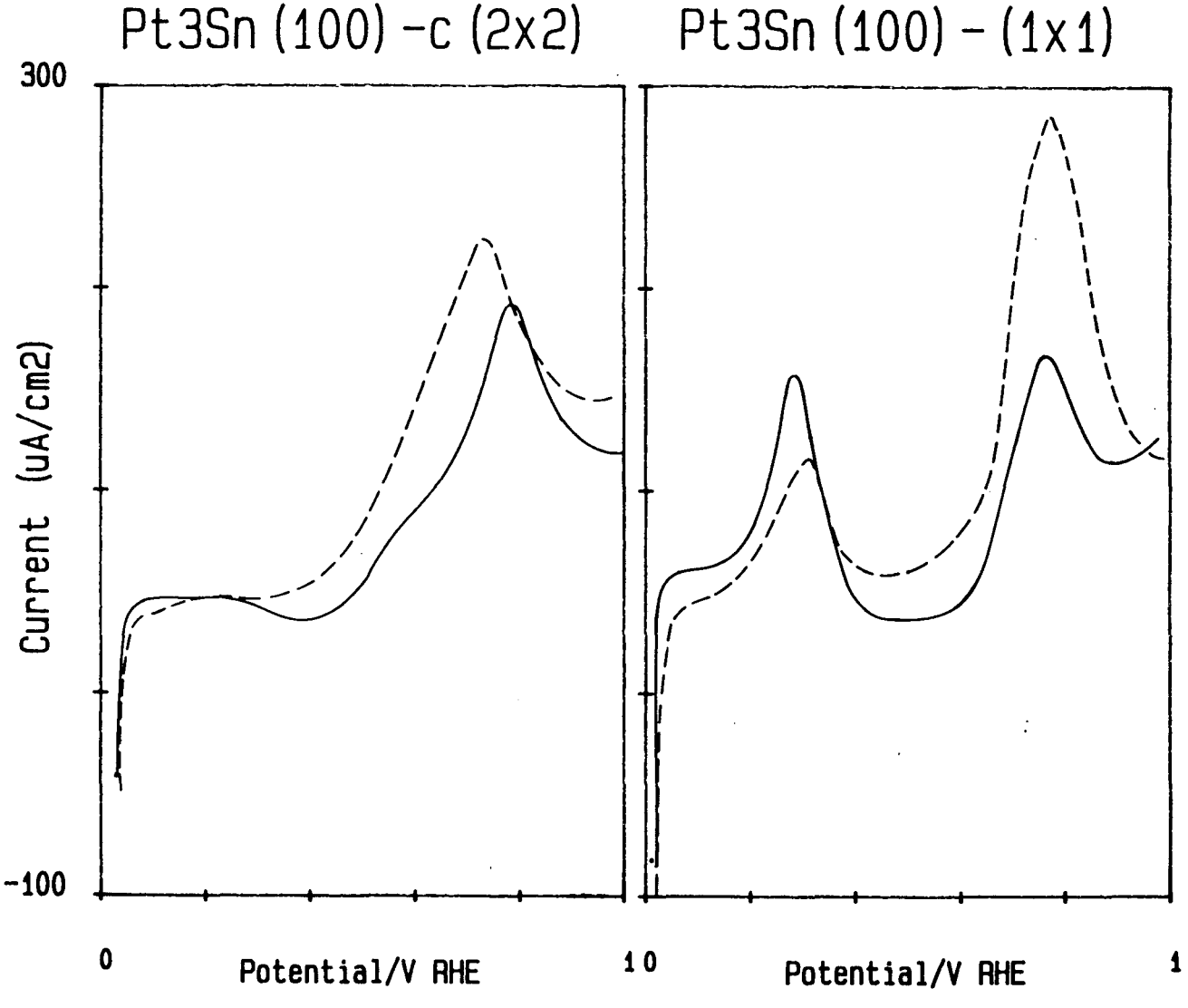

XBL 905 – 6372

Fig. 6

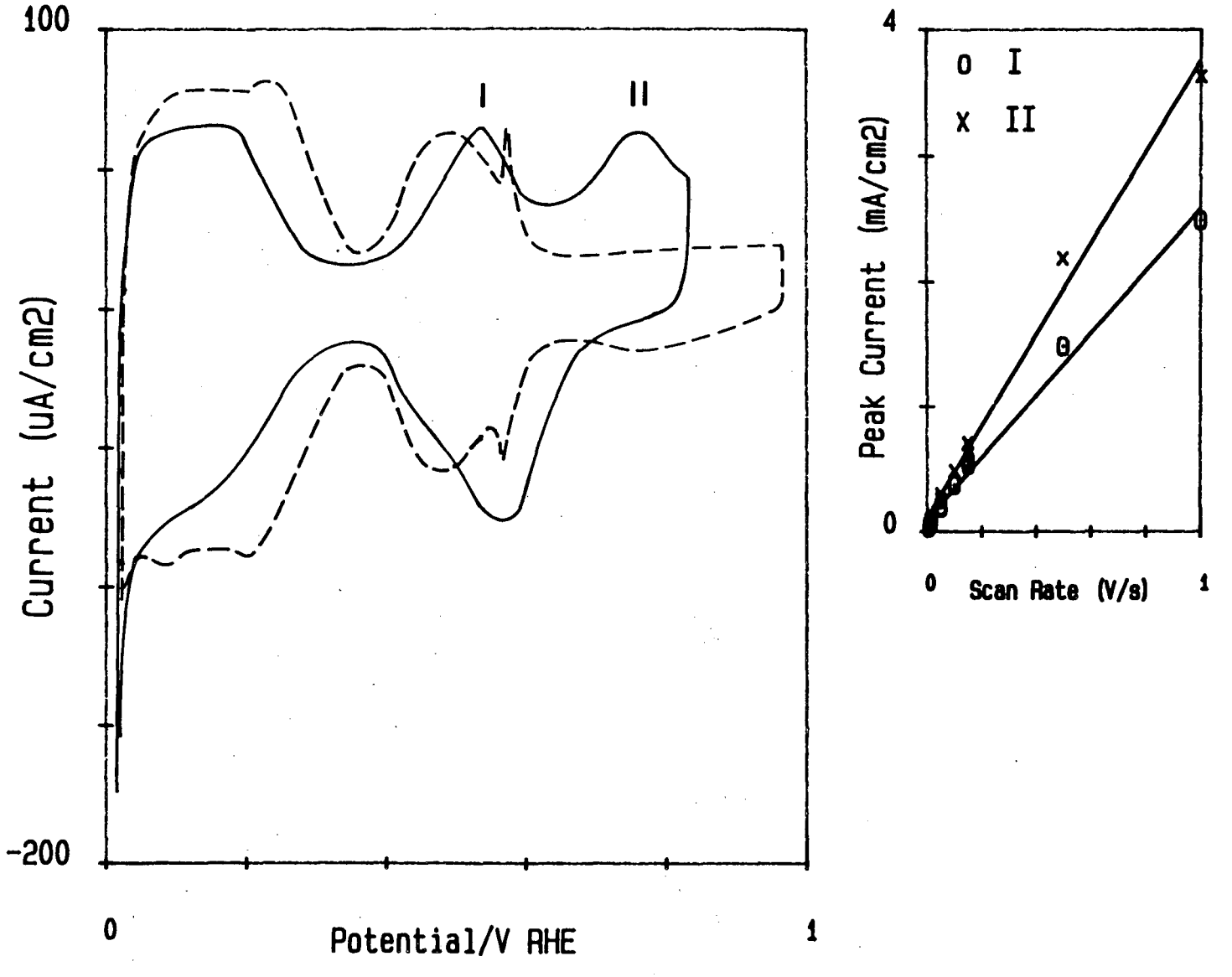

XBL 905 – 6373

Fig. 7

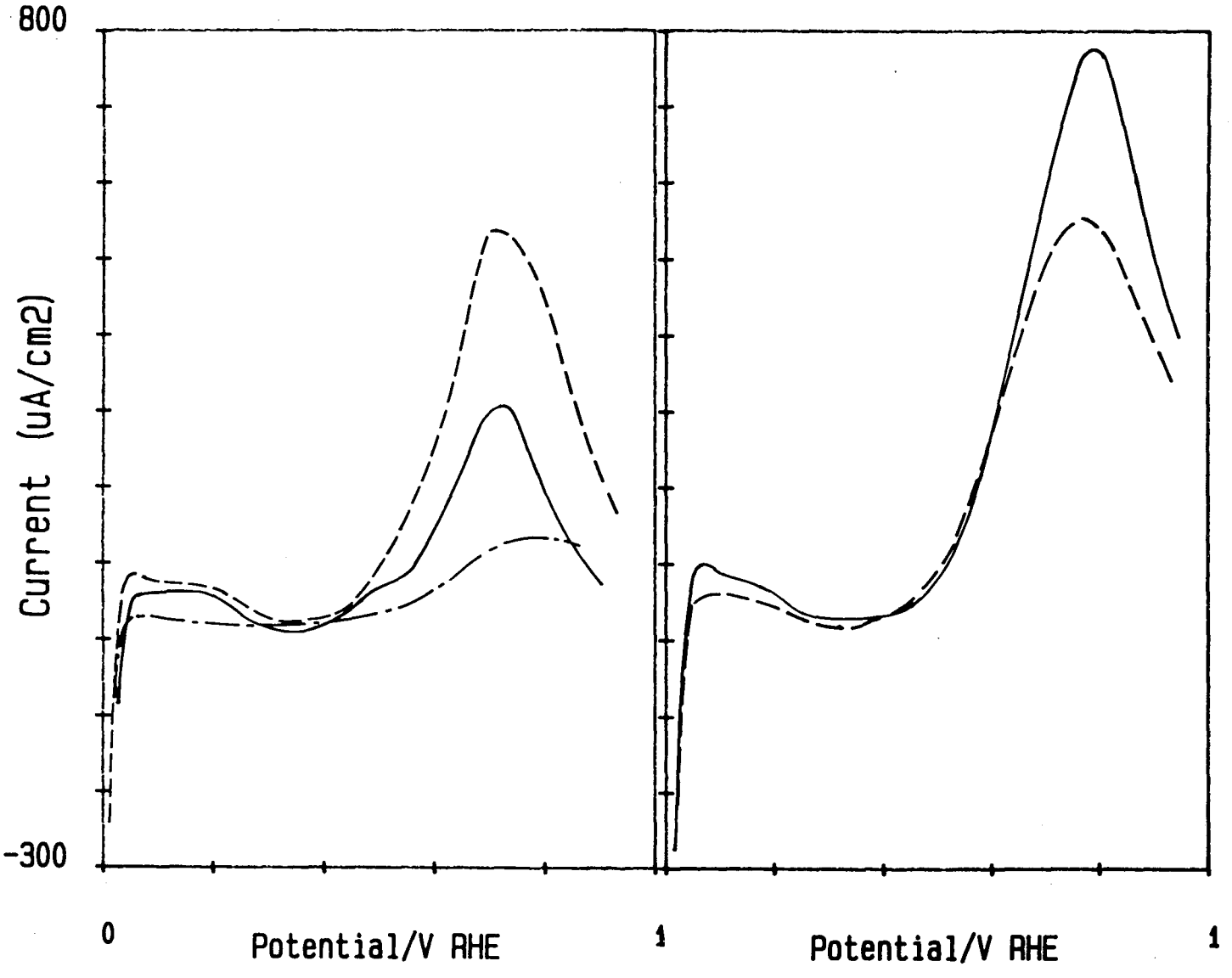

XBL 905 – 6369

Fig. 8

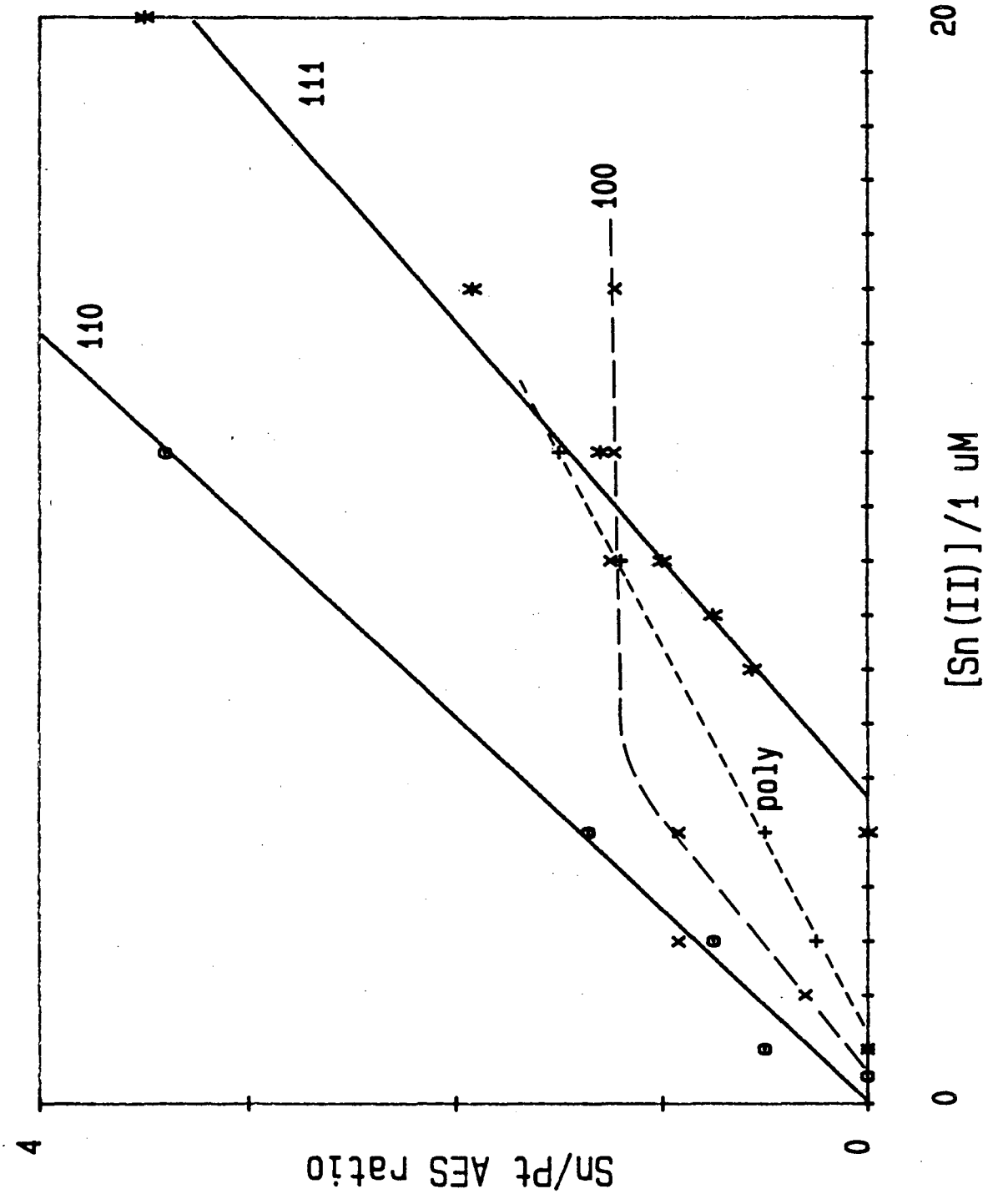

XBL 906-2101

Fig. 9

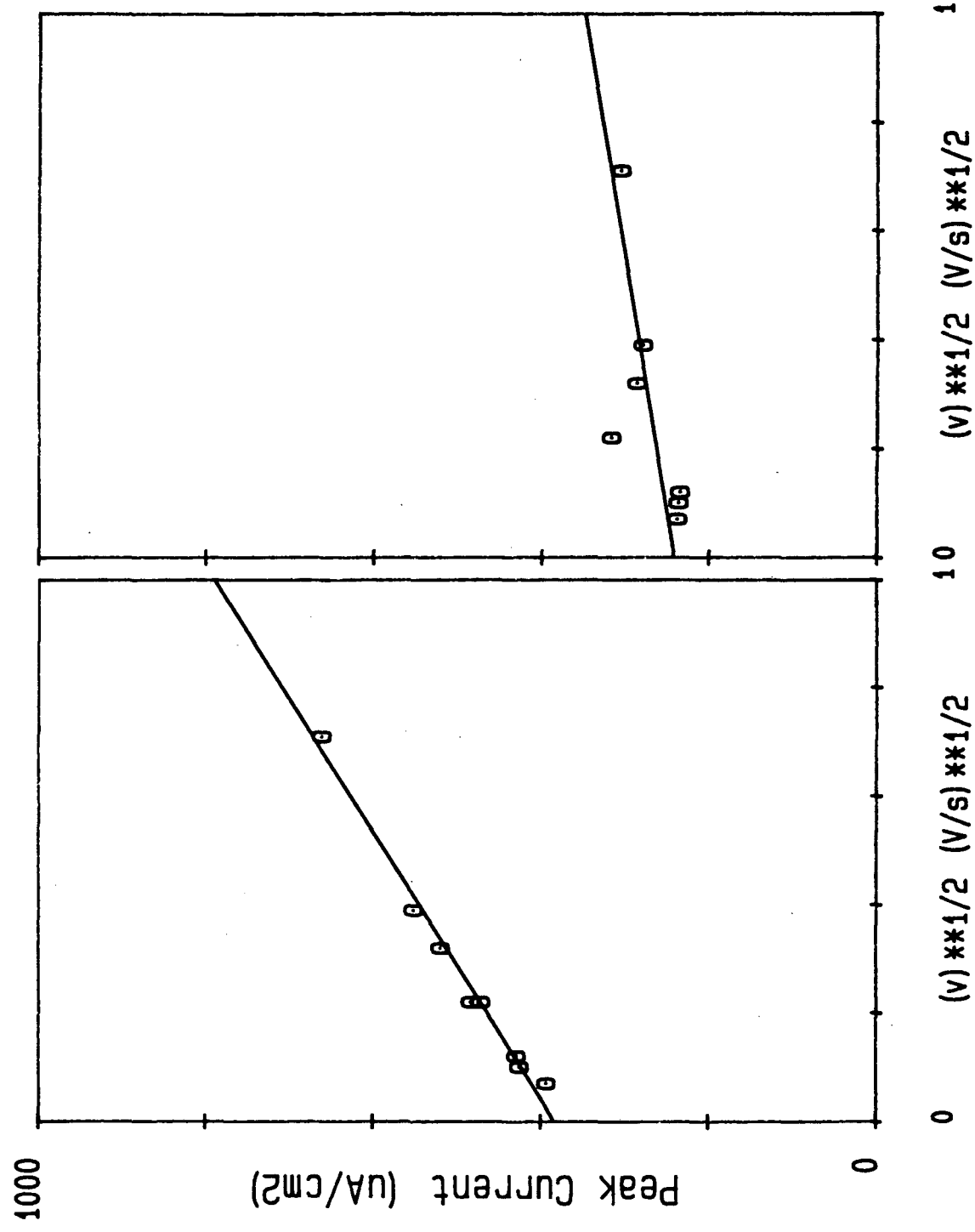

XBL 905-1716

Fig. 10

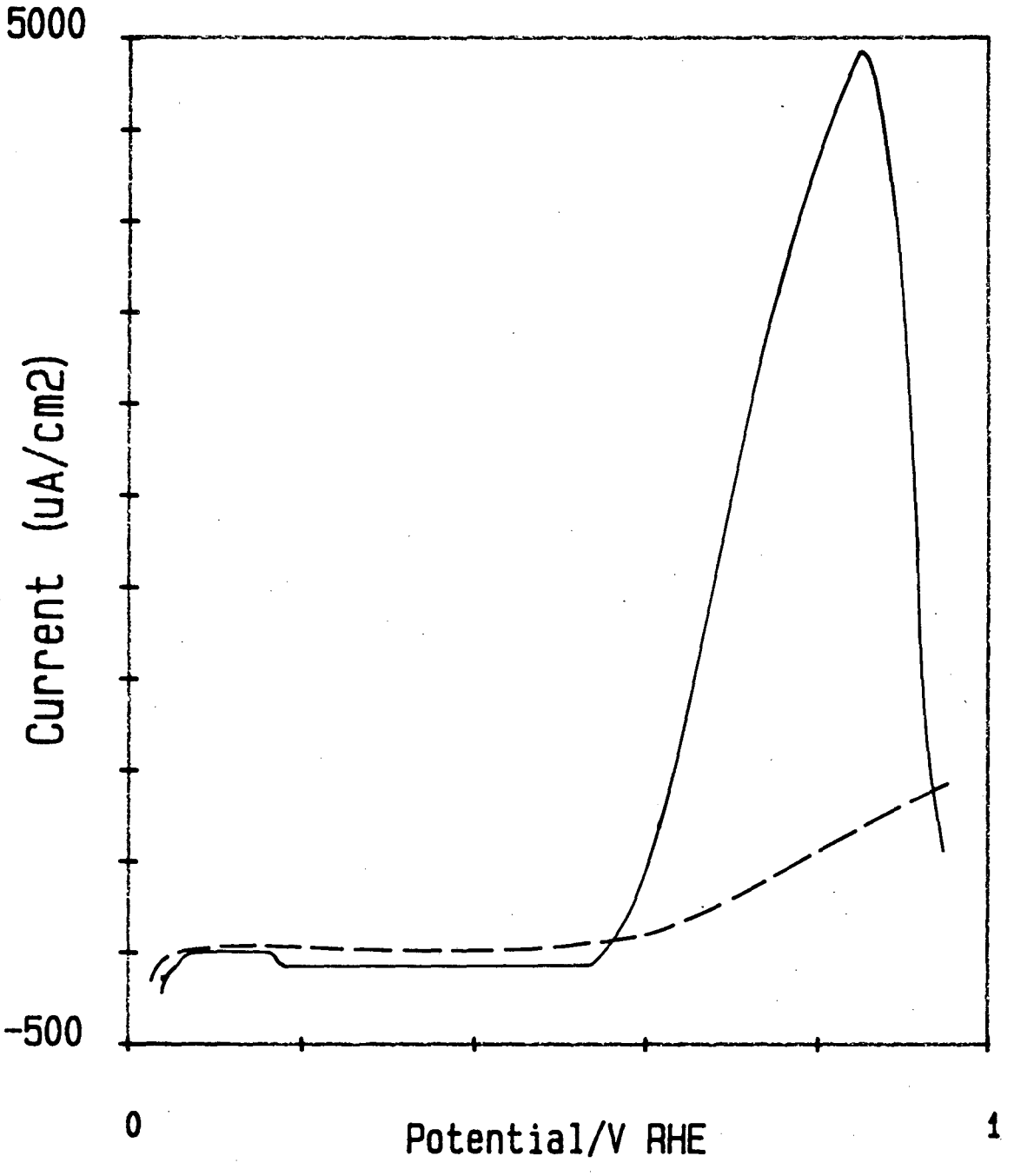

XBL 905 –6374

Fig. 11

REFERENCES

[1] (a) Gilman, S.; Breiter, M.W. *J. Electrochem. Soc.*, **1962**, *109*, 1099. (b) Buck, R.P.; Griffith, L.R. *J. Electrochem. Soc.*, **1962**, *109*, 1005.

[2] Adzic, R. In *Adv. in Electrochem. and Electrochem. Engr.*, Gerischer, H., ed.; Wiley-Interscience: New York, 1984, Vol. 13, pp. 159-260.

[3] Janssen, M.M.P.; Moolhuysen, J. *Electrochim. Acta*, **1976**, *21*, 869.

[4] Watanabe, M.; Furuuchi, Y.; Motoo, S. *J. Electroanal. Chem.*, **1985**, *191*, 367.

[5] (a) Cathro, K.J. *J. Electrochem. Soc.*, **1969**, *116*, 1608. (b) Shropshire, J.A. *J. Electrochem. Soc.*, **1965**, *112*, 465. (c) Shropshire, J.A. *J. Electrochem. Soc.*, **1967**, *114*, 773.

[6] (a) Janssen, M.M.P.; Moolhuysen, J. *Electrochim. Acta*, **1976**, *21*, 861. (b) Janssen, M.M.P.; Moolhuysen, J. *J. Catal.*, **1977**, *46*, 289.

[7] Szabo, S. *J. Electroanal. Chem.*, **1984**, *172*, 359.

[8] Haner, A.N.; Ross, P.N.; Bardi, U *Surface Sci.*, in press.

[9] Heppler, W. LBL Pub. 3078.

[10] Wagner, F.; Ross, P.N. In *Adv. in Electrochem. and Electrochem. Engr.*, Gerischer, H., ed.; Wiley-Interscience: New York, 1984, Vol. 13, pp. 69-112.

[11] Wagner, F.; Ross, P.N. *J. Electroanal. Chem.*, **1988**, *250*, 301.

[12] Pourbaix, M. In *Atlas of Electrochemical Equilibria in Aqueous Solutions*; Pergamon Press: New York, 1966, pp. 475-486.

[13] Wagner, F.T.; Ross, P.N. *Surface Sci.* **1985**, 160, 305.

[14] Bittins-Cattaneo, B.; Iwasita, T. *J. Electroanal. Chem.*, **1987**, *238*, 151.

[15] Sobkowski, J.; Franaszczuk, K.; Piasecki, A. *J. Electroanal. Chem.*, **1985**, *196*, 145.

[16] (a) Bard, A.J.; Faulkner, L.R. In *Electrochemical Methods*, J. Wiley & Sons: NY, 1980. (b) Dimensionless current-potential curves for a generic irreversible reaction, $R = O + ne^-$, using a Butler-Volmer rate expression of the form $C_R^m\ k_s \exp [- (\alpha nF/RT)(E-E^o)]$, which has exactly the same form as in the classical LSV theory in [16a] for $m = 1$, were provided to us by Prof. Dennis Evans, University of Delaware. They showed that the peak current is proportional to $\sqrt{\upsilon}$ and is comparable in magnitude to the peak current for a first-order reaction.

[17] Clavilier, J.; Lamy, C.; Leger, J.M. *J. Electroanal. Chem.*, **1981**, *125*, 249.

[18] D'Agostino, A.T.; Ross, P.N. *Surface Sci.*, **1987**, *185*, 88.

[19] Zei, M.S.; Lempfuhl, G.; Kolb, D.M. *Surface Sci.*, **1989**, *221*, 23.

[20] *Handbook of Auger Electron Spectroscopy*, Physical Electronics Industries, Inc., Eden Prairie, MN, 1976.

[21] Berlowitz, P., Peden, D., and Goodman, D., In *Physical and Chemical Properties of Thin Metal Overlayers and Alloy Surfaces*, Zehner, D.; Goodman, D., Eds.; The Materials Research Society: Pittsburgh, PA, 1987, Vol. 83, p. 161.; and other papers in this volume.

[22] Parsons, R.; VanderNoot T. *J. Electroanal. Chem.*, **1988**, *257*, 9.; and papers therein.

[23] (a) Breiter, M.W. *J. Electroanal. Chem.*, **1967**, *14*, 407. (b) Breiter, M.W. *J. Electroanal. Chem.*, **1967**, *15*, 221.

[24] Andrew, M.R.; Drury, J.S.; McNicol, B.D.;Pinnington, C.D.; Short, R.T. *J. Appl. Electrochem.*, **1976**, *6*, 99.

[25] (a) Motoo, S.; Watanabe, M. *J. Electroanal. Chem.*, **1976**, *69*, 429. (b) Furuya, N.; Motoo, S. *J. Electroanal. Chem.*, **1979**, *98*, 195.

[26] Angerstein-Kozlowska, H.; MacDougal, D.; Conway, B.E. *J. Electrochem. Soc.*, **1973**, *120*, 756.

[27] Beden, B; Kadirgan, F.; Lamy, C; Leger, J.M. *J. Electroanal. Chem.*, **1981**, *127*, 75.

[28] Beden, B.; Lamy, C.; Bewick, A.; Kunimatsu, K. *J. Electroanal. Chem.*, **1981**, *121*, 343.

[29] Castro Luna, A.; Iwasita, T.; Vielstich, W. *J. Electroanal. Chem.*, **1985**, *196*, 301.

[30] Kubota, M. *Inorg. Chem.*, **1990**, *29*, 574.

[31] Roshchupkina, L.I.; Stekolnikov, Y.A.; Altukhov, V.K. *Soviet Electrochemistry*, **1989**, *25*, 343.

Table 1. Auger peak height ratios on platinum surfaces emersed from 25 mM H_2SO_4 containing various amount of Sn(II).

Description	Sn/Pt*	O/Sn
Pt(111)/8 μM Sn(II)	0.56	1
Pt(111)/9 μM Sn(II)	0.75	0.83
Pt(111)/12 μM Sn(II)	1.3	0.75
Pt(111)/20 μM Sn(II)	3.5	0.74
Pt(110)/5 μM Sn(II)	0.75	0.87
Pt(110)/12 μM Sn(II)	3.4	0.71
Pt(110)/80 μM Sn(II)	10.5	0.85
Pt(100)/2 μM Sn(II)	0.3	1
Pt(100)/3 μM Sn(II)	0.92	1
Pt(100)/12 μM Sn(II)	1.23	0.72
Poly Pt/5 μM Sn(II)	0.5	0.83
Poly Pt/10 μM Sn(II)	1.2	0.63
Poly Pt/12 μM Sn(II)	1.5	0.67

* Peak height ratios are not corrected for relative atomic sensitivity factors.

LAWRENCE BERKELEY LABORATORY
UNIVERSITY OF CALIFORNIA
INFORMATION RESOURCES DEPARTMENT
BERKELEY, CALIFORNIA 94720